Acoustic multipole sources for the lattice Boltzmann method

Erlend Magnus Viggen*
Department of Electronics and Telecommunications, NTNU, 7034 Trondheim, Norway
(Received 20 November 2012; published 22 February 2013)

By including an oscillating particle source term, acoustic multipole sources can be implemented in the lattice Boltzmann method. The effect of this source term on the macroscopic conservation equations is found using a Chapman-Enskog expansion. In a lattice with q particle velocities, the source term can be decomposed into q orthogonal multipoles. More complex sources may be formed by superposing these basic multipoles. Analytical solutions found from the macroscopic equations and an analytical lattice Boltzmann wavenumber are compared with inviscid multipole simulations, finding very good agreement except close to singularities in the analytical solutions. Unlike the BGK operator, the regularized collision operator is proven capable of accurately simulating two-dimensional acoustic generation and propagation at zero viscosity.

DOI: 10.1103/PhysRevE.87.023306 PACS number(s): 47.11.−j, 43.20.Rz

I. INTRODUCTION

The lattice Boltzmann (LB) method is a relatively recent advance in computational fluid dynamics, which differs from traditional methods in that it solves the equations of fluid dynamics indirectly using a straightforward discretization of the Boltzmann equation [1]. It has recently also been applied to practical cases in acoustics [2–4] and aeroacoustics [5–7].

This article describes a new method to generate acoustic multipole sources in LB simulations. Acoustic monopole point sources have previously been implemented by completely replacing the particle distribution in a node with an equilibrium distribution having a specified oscillating density [8–13]. In this article we take a different approach by adding a particle source term to the LB equation. Unlike the previous method, the new method does not unphysically disturb the underlying flow, and it also allows dipoles, quadrupoles, and complex multipole superpositions.

II. LATTICE BOLTZMANN WITH OSCILLATING SOURCE TERM

The LB method works by evolving the distribution function $f_i(\mathbf{x},t)$ on a square numerical grid. This function represents the density of particles with position $\mathbf{x}$ and velocity $\boldsymbol{\xi}_i$ at time t. The velocities $\boldsymbol{\xi}_i$ and their associated distribution functions f_i are restricted to a discrete set. From the moments of f_i we can find the macroscopic quantities of density $\rho(\mathbf{x},t) = \sum_i f_i(\mathbf{x},t)$ and momentum density $\rho\mathbf{u}(\mathbf{x},t) = \sum_i \boldsymbol{\xi}_i f_i(\mathbf{x},t)$.

f_i is evolved using the lattice Boltzmann equation,

$$f_i(\mathbf{x}+\boldsymbol{\xi}_i,t+1) = f_i(\mathbf{x},t) + \Omega_i(\mathbf{x},t) + s_i(\mathbf{x},t), \tag{1}$$

where s_i is the aforementioned particle source term, and Ω_i is a collision operator. Most common is the BGK operator, which relaxes f_i to an equilibrium

$$f_i^{(0)} = \rho w_i \left(1 + \frac{\boldsymbol{\xi}_i\cdot\mathbf{u}}{c_0^2} + \frac{(\boldsymbol{\xi}_i\cdot\mathbf{u})^2}{2c_0^4} - \frac{\mathbf{u}\cdot\mathbf{u}}{2c_0^2}\right), \tag{2}$$

with a relaxation time τ,

$$\Omega_i = -\frac{1}{\tau}\left(f_i - f_i^{(0)}\right). \tag{3}$$

In Eq. (2), c_0 is the inviscid speed of sound and w_i is a set of weighting coefficients; both depend on the choice of velocity set $\boldsymbol{\xi}_i$.

This article primarily uses the regularized collision operator [14], which behaves similarly to BGK but suppresses nonhydrodynamic moments of f_i by relaxing them to equilibrium in each time step. It may thus be seen as a conceptually simple, efficient, and generally applicable multiple relaxation time operator, which improves on the accuracy and stability of the BGK operator, in particular at low viscosities. The regularized collision operator is given by

$$\Omega_i = \frac{\left(1-\frac{1}{\tau}\right)w_i}{2c_0^4}\sum_j \left(\xi_{i\alpha}\xi_{i\beta} - c_0^2\delta_{\alpha\beta}\right)\xi_{j\alpha}\xi_{j\beta}f_j^{\mathrm{neq}} - f_i^{\mathrm{neq}}, \tag{4}$$

where $f_i^{\mathrm{neq}} = f_i - f_i^{(0)}$. In this notation, Greek indices indicate vector or tensor components, and repeated Greek indices in a term imply a summation (i.e., $a_\alpha b_\alpha = \sum_\alpha a_\alpha b_\alpha$). $\delta_{\alpha\beta}$ is the Kronecker δ.

The source term's effect on the conservation equations can be analyzed using a Taylor and Chapman-Enskog expansion [15]. Because Eqs. (3) and (4) have the same hydrodynamic moments [14], performing the analysis using Eq. (3) gives results that are valid for both. f_i is expanded around $f_i^{(0)}$ in orders of the Knudsen number, and s_i and the derivatives are also similarly expanded:

$$f_i = f_i^{(0)} + \epsilon f_i^{(1)} + \epsilon^2 f_i^{(2)} + \ldots, \quad s_i = \epsilon s_i,$$
$$\partial_t = \epsilon\partial_{t_1} + \epsilon^2\partial_{t_2}, \quad \partial_\alpha = \epsilon\partial_\alpha.$$

Here, ϵ is an expansion parameter indicating the order of the Knudsen number. After inserting Eq. (3) into Eq. (1), Taylor expanding, collecting terms according to their Knudsen number order, and performing some algebra, we find

$$\left(\partial_{t_1} + \partial_\alpha\xi_{i\alpha}\right)f_i^{(0)} = -\frac{1}{\tau}f_i^{(1)} + s_i \tag{5}$$

*erlend.viggen@ntnu.no

at $O(\epsilon)$, and

$$\partial_{t_2} f_i^{(0)} + \left(\partial_{t_1} + \partial_\alpha \xi_{i\alpha}\right)\left(1 - \frac{1}{2\tau}\right) f_i^{(1)} = -\frac{1}{\tau} f_i^{(2)} - \frac{1}{2}\left(\partial_{t_1} + \partial_\alpha \xi_{i\alpha}\right) s_i \tag{6}$$

at $O(\epsilon^2)$. Then we define the monopole, dipole, and quadrupole moments of s_i, respectively, as

$$S_0 = \sum_i s_i, \quad S_\alpha = \sum_i \xi_{i\alpha} s_i, \quad S_{\alpha\beta} = \sum_i \xi_{i\alpha}\xi_{i\beta} s_i. \tag{7}$$

Finally, combining the different moments of Eqs. (5) and (6) [1,15], we end up with a modified mass conservation equation,

$$\frac{\partial \rho}{\partial t} + \frac{\partial \rho u_\alpha}{\partial x_\alpha} = S_0 - \frac{1}{2}\left(\frac{\partial S_0}{\partial t} + \frac{\partial S_\alpha}{\partial x_\alpha}\right), \tag{8}$$

and a modified momentum conservation equation,

$$\begin{aligned}\frac{\partial \rho u_\alpha}{\partial t} + \frac{\partial \rho u_\alpha u_\beta}{\partial x_\beta} + \frac{\partial p}{\partial x_\alpha} - \frac{\partial}{\partial x_\beta}\nu\left(\frac{\partial u_\beta}{\partial x_\alpha} + \frac{\partial u_\alpha}{\partial x_\beta}\right) \\ = \left(1 - \frac{1}{2}\frac{\partial}{\partial t}\right) S_\alpha - \tau \frac{\partial S_{\alpha\beta}}{\partial x_\beta} \\ + \left(\tau - \frac{1}{2}\right)\frac{\partial}{\partial x_\beta}\left(c_s^2 \delta_{\alpha\beta} S_0 + u_\alpha S_\beta + u_\beta S_\alpha - u_\alpha u_\beta S_0\right).\end{aligned} \tag{9}$$

Here, we have a pressure $p = c_0^2 \rho$, a kinematic shear viscosity $\nu = (\tau - \frac{1}{2})c_0^2 \rho$, and a bulk viscosity of $2\nu/3$. The $O(u^3)$ error term [1] has been neglected.

An inhomogeneous linear wave equation can be derived from these conservation equations. In the $\tau \to \frac{1}{2}$ limit, corresponding to the low viscosities commonly chosen for LB acoustics [3,5], this equation is

$$\frac{1}{c_0^2}\frac{\partial^2 p'}{\partial t^2} - \nabla^2 p' = \left(1 - \frac{1}{2}\frac{\partial}{\partial t}\right)\frac{\partial S_0}{\partial t} - \frac{\partial S_\alpha}{\partial x_\alpha} + \tau \frac{\partial^2 S_{\alpha\beta}}{\partial x_\alpha \partial x_\beta}, \tag{10}$$

where the acoustic pressure $p'(\mathbf{x},t) = p(\mathbf{x},t) - p_0$ is the pressure's deviation from a rest state. Unlike when this equation is derived in the continuous Boltzmann equation case [16], $S_{\alpha\beta}$ does not fully disappear with viscosity. This is a fortuitous consequence of the discretization error inherent in the lattice Boltzmann scheme.

In the simplified case of a time-harmonic source term with angular frequency ω, the solution to this equation can be found using standard methods [17] to be

$$p'(\mathbf{x},t) = \mathrm{Re}\left\{\int\left[\left(i\omega - \frac{(i\omega)^2}{2}\right) S_0(\mathbf{y}) G(\mathbf{x}-\mathbf{y},t) - S_\alpha(\mathbf{y})\frac{\partial G(\mathbf{x}-\mathbf{y},t)}{\partial x_\alpha} + \tau S_{\alpha\beta}(\mathbf{y})\frac{\partial^2 G(\mathbf{x}-\mathbf{y},t)}{\partial x_\alpha \partial x_\beta}\right]\mathrm{d}\mathbf{y}\right\}, \tag{11}$$

where $G(\mathbf{x},t)$ is the time-harmonic Green's function. The three terms in the integral represent monopoles, dipoles, and quadrupoles, respectively. For the two-dimensional case used in the following sections,

$$G(\mathbf{x},t) = \frac{1}{4i} H_0^{(2)}(k|\mathbf{x}|)\, e^{i\omega t}, \tag{12}$$

where $H_n^{(2)}$ is the nth order Hankel function of the second kind and $k = \omega/c_0$ is the wavenumber [18].

However, waves in LB simulations have nonideal wavenumbers, due to discretization errors and viscous effects [19,20]. It has been shown that linear LB wave propagation can be formulated as an eigenvalue problem [1,19]. From the corresponding characteristic polynomial,

$$\left|\frac{1}{3}\begin{bmatrix} e^{-i\hat{k}}(3-1/\tau) & e^{-i\hat{k}}/2\tau & -e^{-i\hat{k}}/\tau \\ 2/\tau & 3-1/\tau & 2/\tau \\ -e^{i\hat{k}}/\tau & e^{i\hat{k}}/2\tau & e^{i\hat{k}}(3-1/\tau)\end{bmatrix} - e^{i\omega}\mathbf{I}\right| = 0,$$

an analytical LB wavenumber including the aforementioned effects can be found to be

$$\hat{k} = i\ln\{[3\tau(\zeta^2 - \zeta + 1 - \zeta^{-1}) + \zeta - 2 + 3\zeta^{-1} + \sqrt{3}\zeta^{-1}\sqrt{\Xi}]/[4 + 6\tau(\zeta - 1) - 2\zeta]\}, \tag{13}$$

where the shorthand $\zeta = e^{i\omega}$ has been used, and

$$\Xi = (\zeta + 1)(\zeta - 1)^2(\tau\zeta + 1 - \tau)(3\tau\zeta^2 - \zeta + 3 - 3\tau).$$

This wavenumber is used in this article when comparing analytical and numerical solutions.

III. MULTIPOLE BASIS

For a velocity set with q velocities, s_i can be seen as a q-dimensional vector, which can be found from a q-dimensional orthogonal basis M_j as $s_i(\mathbf{x},t) = A_{ij} M_j(\mathbf{x},t)$. A_{ij} can be chosen so that each component of M_j represents the strength of a particular multipole. As all LB velocity sets are symmetric and have an odd number of velocities, one reasonable choice is to have one monopole in addition to $(q-1)/2$ pairs of oddly symmetric dipoles and evenly symmetric longitudinal quadrupoles; one such pair for each pair of opposing velocities $\boldsymbol{\xi}_i$.

For the two-dimensional D2Q9 lattice, where

$$\boldsymbol{\xi}_i = \begin{cases} (0,\,0) & \text{for } i = 0, \\ \left[\sin(\frac{i-1}{2}\pi),\ \cos(\frac{i-1}{2}\pi)\right] & \text{for } i = 1\text{–}4, \\ \sqrt{2}\left[\sin(\frac{2i-1}{4}\pi),\ \cos(\frac{2i-1}{4}\pi)\right] & \text{for } i = 5\text{–}8, \end{cases}$$

$$w_i = \begin{cases} 4/9 & \text{for } i = 0, \\ 1/9 & \text{for } i = 1\text{–}4, \\ 1/36 & \text{for } i = 5\text{–}8, \end{cases} \tag{14}$$

and $c_0 = 1/\sqrt{3}$, the source term can be decomposed in this way as

$$\begin{bmatrix} s_0 \\ s_1 \\ s_2 \\ s_3 \\ s_4 \\ s_5 \\ s_6 \\ s_7 \\ s_8 \end{bmatrix} = \begin{bmatrix} w_0 & 0 & 0 & -1 & -1 & 0 & 0 & -\frac{1}{2} & -\frac{1}{2} \\ w_1 & \frac{1}{2} & 0 & \frac{1}{2} & 0 & 0 & 0 & 0 & 0 \\ w_2 & 0 & \frac{1}{2} & 0 & \frac{1}{2} & 0 & 0 & 0 & 0 \\ w_3 & -\frac{1}{2} & 0 & \frac{1}{2} & 0 & 0 & 0 & 0 & 0 \\ w_4 & 0 & -\frac{1}{2} & 0 & \frac{1}{2} & 0 & 0 & 0 & 0 \\ w_5 & 0 & 0 & 0 & 0 & \frac{1}{\sqrt{8}} & 0 & \frac{1}{4} & 0 \\ w_6 & 0 & 0 & 0 & 0 & 0 & \frac{1}{\sqrt{8}} & 0 & \frac{1}{4} \\ w_7 & 0 & 0 & 0 & 0 & \frac{-1}{\sqrt{8}} & 0 & \frac{1}{4} & 0 \\ w_8 & 0 & 0 & 0 & 0 & 0 & \frac{-1}{\sqrt{8}} & 0 & \frac{1}{4} \end{bmatrix} \begin{bmatrix} M_0 \\ M_x \\ M_y \\ M_{xx} \\ M_{yy} \\ M_{x'} \\ M_{y'} \\ M_{x'x'} \\ M_{y'y'} \end{bmatrix}. \tag{15}$$

The monopole has been chosen so that particles are added at equilibrium. An x'-y' coordinate system, rotated $\pi/4$ to the x-y one, has been defined for the diagonal dipoles and quadrupoles. Table I shows how these nine multipoles map onto the moments defined in Eq. (7). It indicates that lateral quadrupoles can be made by superposition of the diagonal longitudinal quadrupoles: subtracting $M_{y'y'}$ from $M_{x'x'}$ and normalizing.

IV. NUMERICAL VERIFICATION

To determine the correctness of the radiated fields of these multipoles, a multipole point source was placed at $\mathbf{x} = 0$ in a system originally at rest with a density ρ_0. The simulated radiated field was compared with the corresponding analytical solution for several representative multipoles. The simulations presented in this article were performed at zero viscosity; i.e., $\tau = \frac{1}{2}$. To avoid ripple caused by sudden onset of the source, the source's amplitude was multiplied with an envelope function

$$E(t) = \begin{cases} 0 & \text{for } t \leqslant 0, \\ \frac{1}{2} - \frac{1}{2}\cos(\omega t/2) & \text{for } 0 \leqslant t \leqslant 2\pi/\omega, \\ 1 & \text{for } 2\pi/\omega \leqslant t. \end{cases} \tag{16}$$

The point source was left to radiate waves until the first wavefront neared the edge of the simulated system, at which point the simulation was stopped and the results were compared with the analytical solution.

To avoid nonlinearities affecting the results, the LB method was linearized by removing the $O(u^2)$ terms in Eq. (2). As the resulting dynamics and macroscopic equations are linear, this allows the use of a complex phasor source, which in turn allows a more simple and accurate analysis. The real part of the complex radiated field represents its physical value, and the magnitude represents its amplitude.

TABLE I. Nonzero moments of the D2Q9 basis multipoles M_j.

	M_0	M_x	M_y	M_{xx}	M_{yy}	$M_{x'}$	$M_{y'}$	$M_{x'x'}$	$M_{y'y'}$
S_0	1								
S_x		1				$\frac{1}{\sqrt{2}}$	$-\frac{1}{\sqrt{2}}$		
S_y			1			$\frac{1}{\sqrt{2}}$	$\frac{1}{\sqrt{2}}$		
S_{xx}	c_0^2			1				$\frac{1}{2}$	$\frac{1}{2}$
S_{yy}	c_0^2				1			$\frac{1}{2}$	$\frac{1}{2}$
S_{xy}								$\frac{1}{2}$	$-\frac{1}{2}$
S_{yx}								$\frac{1}{2}$	$-\frac{1}{2}$

For a two-dimensional complex time-harmonic multipole point source, $s_i(\mathbf{x},t) = s_i\delta(\mathbf{x})\,e^{i\omega t}$, at $\tau = \frac{1}{2}$, Eq. (11) becomes

$$p'(\mathbf{x},t) = i\omega S_0 G(\mathbf{x},t) - S_\alpha \frac{\partial G(\mathbf{x},t)}{\partial x_\alpha} + \frac{1}{2}\left(S_{\alpha\beta} - c_0^2\delta_{\alpha\beta}S_0\right)\frac{\partial^2 G(\mathbf{x},t)}{\partial x_\alpha \partial x_\beta}, \tag{17}$$

because from Eq. (12),

$$(i\omega)^2 G(\mathbf{x},t) = \frac{-\omega^2}{4i} H_0^{(2)}(k|\mathbf{x}|)\,e^{i\omega t} = \left(\frac{\omega}{k}\right)^2 \frac{\partial^2 G(\mathbf{x},t)}{\partial x_\alpha \partial x_\alpha}.$$

The three right-hand terms in Eq. (17) are only affected by monopole, dipole, and quadrupole multipole strengths, respectively; Table I indicates that the two components of the third term cancel for M_0.

The waves radiated from three representative multipoles, simulated with both the BGK and regularized collision operators at a source frequency $\omega = 2\pi/25$, are compared with the analytical solution from Eq. (17) in Fig. 1. While neither collision operator is unstable for this simulation, the BGK LB results are heavily affected by spurious oscillations, particularly for the higher-order multipoles. On the other hand, the regularized LB results show no such oscillations and are only significantly in error very close to the point source. At this point there is a singularity in the analytical solution that cannot be captured with any similar discrete simulation methods, such as finite difference time domain methods. Similar errors were also reported in two and three dimensions for the previous LB monopole point source method [9]. Also, since we are comparing a non-steady-state simulated result and a steady-state analytical solution, there is naturally a discrepancy near the first wavefront; this area is, therefore, not shown in Fig. 1.

The fundamental difference between the two collision operators is that the BGK operator has a relaxation time τ for all moments, while the regularized operator relaxes nonhydrodynamic moments to equilibrium in each time step [14]. At $\tau = \frac{1}{2}$, the BGK operator fully overrelaxes nonhydrodynamic moments in such a way that their amplitude does not decrease. By increasing τ in these simulations, the

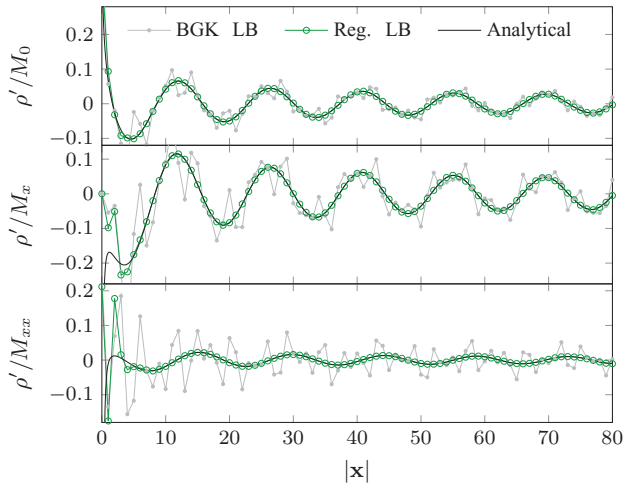

FIG. 1. (Color online) Physical acoustic density $\rho' = \mathrm{Re}(p'/c_0^2)$ normalized by multipole strength M_j against distance $|\mathbf{x}|$ to point source. Results were measured along the x axis. Top to bottom: monopole, x dipole, xx quadrupole.

spurious oscillations in the BGK results are reduced and localized to the region around the source. This indicates that the difference shown in Fig. 1 between the two operators is caused by nonhydrodynamic moments generated in the source node. The regularized collision operator at $\tau = \frac{1}{2}$ is used exclusively in the remainder of this article.

In a region well away from the source and the first wavefront, the q-norm of the relative error [21] of the monopole pressure amplitude is

$$\|e\|_q = \left(\frac{1}{\lambda^2} \sum_{|\mathbf{x}|=\lambda}^{3\lambda} \left| \frac{|p'^*| - |p'|}{|p'|} \right|^q \right)^{1/q}, \qquad (18)$$

where $\lambda = 2\pi c_0/\omega$ is the wavelength, p' is the analytical solution, and p'^* is the simulated solution. The 1- and 2-norms were found for a number of different resolutions, and the results are shown as function of the spatial resolution $1/\lambda$ in Fig. 2. The overall convergence of the radiated wave is clearly seen to be second order, the same order as the LB method itself.

The directivity at $k|\mathbf{x}| = 25$ of the dipole and the longitudinal and lateral quadrupoles, simulated at $\omega = 2\pi/50$, is shown in Figs. 3(a)–3(c). In all three cases, there is an excellent agreement between the numerical and analytical solutions.

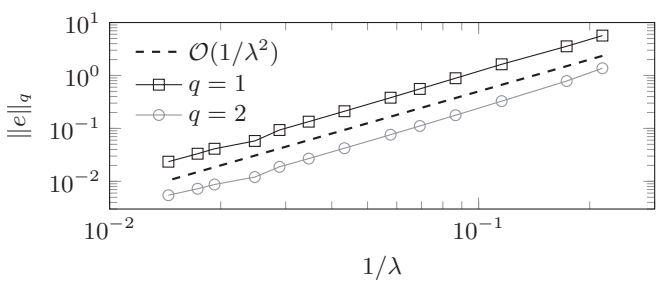

FIG. 2. 1- and 2-norm of the relative error of the monopole pressure amplitude, found by Eq. (18), compared with second-order convergence.

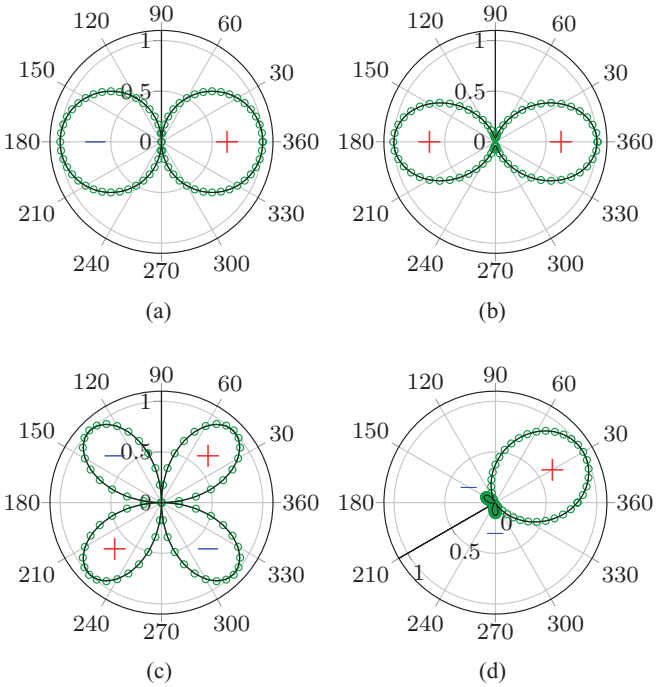

FIG. 3. (Color online) Directivity at $k|\mathbf{x}| = 25$, normalized by the analytical solution. Lobe phase is indicated by plus and minus signs. Circles and lines indicate numerical and analytical solutions, respectively. (a) x dipole; (b) xx quadrupole; (c) xy quadrupole; (d) rotated supercardioid.

The basic multipoles may be superposed to form more complex ones. Rotation by an angle θ may be performed by applying a rotation matrix $\alpha_{ij} = \left[\begin{smallmatrix} \cos\theta & -\sin\theta \\ \sin\theta & \cos\theta \end{smallmatrix}\right]$ to a dipole vector $D_i = \left[\begin{smallmatrix} S_x \\ S_y \end{smallmatrix}\right]$ like $D_i^{\mathrm{rot}} = \sum_j \alpha_{ij} D_j$, or to a quadrupole tensor $Q_{ij} = \left[\begin{smallmatrix} S_{xx} & S_{xy} \\ S_{yx} & S_{yy} \end{smallmatrix}\right]$ like $Q_{ij}^{\mathrm{rot}} = \sum_{m,n} \alpha_{im}\alpha_{jn} Q_{mn}$. Figure 3(d) shows a rotated supercardioid formed by superposing a dipole and a longitudinal quadrupole [22], both normalized to the same amplitude and rotated an angle $\theta = \pi/6$. This composite multipole is highly directive.

V. COMPARISON WITH PREVIOUS METHOD

A previous method for acoustic monopole point sources within the LB domain [8–13] works by replacing the distribution function f_i in the source node in each time step. It is replaced by an equilibrium distribution $f_i^{(0)}$ determined by the velocity $\mathbf{u}$, found from f_i, and a specified oscillating density:

$$\rho = \rho_0 + \rho_{\mathrm{src}} \sin(\omega t). \qquad (19)$$

Thus, the original density and all information contained in f_i^{neq} is overwritten and lost in the source node in each time step. Extending the previous method for dipoles is possible by making $\mathbf{u}$ an oscillating function of time. However, extending it further would not be possible, as the equilibrium distribution it depends on is fully defined by ρ and $\mathbf{u}$.

Unlike the current method described in this article, there have never been found any expressions for the previous method, either regression- or theory-based, to relate the amplitudes and phases of the source node and the radiated

wave. Previous comparisons of the previous method with theory have been done by ad hoc scaling and phase shifting of the analytical solution [8,9]. Thus, we cannot make fair direct quantitative comparisons with theory like in the previous section.

However, the previous method systematically generates errors in the source node. This is most clearly seen in a limiting case where the monopole source strength goes to zero (i.e., $s_i \to 0$ and $\rho_{\mathrm{src}} \to 0$) and there is a background flow field with a density $\rho(\mathbf{x},t) = \rho_0 + \rho'(\mathbf{x},t)$. For the current method, Eq. (1) shows that the effect of the source vanishes. For the previous method, however, Eq. (19) shows that the fixed source node density ρ_0 will result in a relative error $|\rho'/(\rho_0 + \rho')|$. This error will propagate outward, affecting the rest of the flow field.

VI. CONCLUSION

By adding an oscillating particle source term to the LB equation, acoustic multipole sources may be implemented. These may be either spatially distributed or point sources. Comparing simulations of the fields radiated by monofrequency point multipole sources with the corresponding fields predicted by theory, very good agreement is found except in the vicinity of the source node, where there is a singularity in the analytical solution. Similar errors were also reported for a previous LB monopole point source method [9].

In a lattice with q velocities, we suggest using an orthogonal multipole basis of one monopole, $(q-1)/2$ dipoles, and $(q-1)/2$ longitudinal quadrupoles. These fundamental multipoles may be superposed to form more complex sources, such as the highly directive source shown in Fig. 3(d). This could be useful for simulating cases with directed emission of sound in a complex fluid flow.

Because acoustic LB simulations are commonly performed at very low viscosities, i.e., τ close to $\frac{1}{2}$ [3,5], the simulations in this article were performed using the regularized collision operator at the inviscid limit $\tau = \frac{1}{2}$. The simulations prove that the regularized operator allows stable and accurate zero-viscosity LB simulation of some phenomena, at minimum acoustic generation and propagation. For the same case, the BGK operator gives results with very large spurious oscillations unless the viscosity is increased. This is because it does not at all, when $\tau = \frac{1}{2}$, suppress the nonhydrodynamic moments generated by the source node, unlike the regularized operator, which fully suppresses them.

It is worth noting that while monopoles, dipoles, and quadrupoles appear as source terms in the wave equation, higher-order multipoles, such as octupoles, do not. This is also the case when the wave equation is similarly derived from the continuous Boltzmann equation [16]. However, it is likely that such higher-order multipoles would appear in the momentum equation if its derivation were carried to the Burnett level, where the equation contains additional terms with derivatives of higher order. Thus, octupoles, etc., are likely also possible in LB simulations, if the symmetries of the chosen velocity set permit.

Comparison with the derivation based on the continuous Boltzmann equation also shows that the quadrupole strength here is nonzero in the inviscid limit due to a fortuitous discretization error in the lattice Boltzmann scheme. In the continuous case, quadrupoles disappear in this limit.

ACKNOWLEDGMENTS

The author thanks Paul J. Dellar for suggesting how to find Eq. (13).

[1] P. J. Dellar, Phys. Rev. E **64**, 031203 (2001).
[2] H. Kühnelt, in Proceedings of the Stockholm Music Acoustics Conference, August 6–9, 2003 (SMAC 03), Stockholm, pp. 401–404 [http://www.speech.kth.se/smac03/].
[3] A. R. da Silva, G. P. Scavone, and A. Lefebvre, J. Sound Vib. **327**, 507 (2009).
[4] J. M. Buick, M. Atig, D. J. Skulina, D. M. Campbell, J. P. Dalmont, and J. Gilbert, J. Acoust. Soc. Am. **129**, 1261 (2011).
[5] M. Hasert, J. Bernsdorf, and S. Roller, Phil. Trans. R. Soc. A **369**, 2467 (2011).
[6] F. A. van Herpe, S. Vergne, and E. Gaudard, in Proceedings of the Acoustics 2012 Nantes Conference (2012), pp. 1845–1850 [http://www.acoustics2012-nantes.org].
[7] M. Stadler, M. B. Schmitz, P. Ragg, D. M. Holman, and R. Brionnaud, in *2012 Proceedings of the ASME Turbo Expo* (ASME, New York, 2012).
[8] E. M. Viggen, Master's thesis, Norwegian University of Science and Technology (NTNU), 2009 [http://urn.kb.se/resolve?urn=urn:nbn:no:ntnu:diva-6345].
[9] E. M. Viggen, in Proceedings of the 33rd Scandinavian Symposium on Physical Acoustics, 2010 [http://www.iet.ntnu.no/en/groups/akustikk/meetings/SSPA/2010/Viggen].
[10] H. Xu and P. Sagaut, J. Comput. Phys. **230**, 5353 (2011).
[11] E. Vergnault, O. Malaspinas, and P. Sagaut, J. Comput. Phys. **231**, 8070 (2012).
[12] S. Ha, N. Ku, and K.-Y. Lee, in *Proceedings of the 2012 Symposium on Theory of Modeling and Simulation* (Society for Computer Simulation International, San Diego, CA, 2012).
[13] H. Xu, O. Malaspinas, and P. Sagaut, J. Comput. Phys. **231**, 7335 (2012).
[14] J. Lätt and B. Chopard, Math. Comput. Simulation **72**, 165 (2006).
[15] T. Reis and T. N. Phillips, Phys. Rev. E **75**, 056703 (2007).
[16] E. M. Viggen, arXiv:1302.3764 [Proceedings of the 36th Scandinavian Symposium on Physical Acoustics (to be published)].
[17] M. S. Howe, *Theory of Vortex Sound* (Cambridge University Press, Cambridge, 2003), Chaps. 1–2.
[18] P. M. Morse and K. U. Ingard, *Theoretical Acoustics* (McGraw-Hill Book Company, New York, 1968), Chap. 7.
[19] E. M. Viggen, Phil. Trans. R. Soc. A **369**, 2246 (2011).
[20] E. M. Viggen, Commun. Comput. Phys. **13**, 671 (2013).
[21] R. J. LeVeque, *Finite Difference Methods for Ordinary and Partial Differential Equations* (Society for Industrial and Applied Mathematics, Philadelphia, PA, 2007), Appendix A.
[22] J. L. Butler, A. L. Butler, and J. A. Rice, J. Acoust. Soc. Am. **115**, 658 (2004).